Parallels between Metal-Ligand Cooperativity and Frustrated Lewis Pairs

Habraken, Evi

2019-05-26

Habraken , E , Jupp , A , Brands , M , Nieger , M , Ehlers , A & Slootweg , C 2019 , ' Parallels between Metal-Ligand Cooperativity and Frustrated Lewis Pairs ' , European Journal of Inorganic Chemistry , no. 19 , pp. 2436-2442 . https://doi.org/10.1002/ejic.201900169

http://hdl.handle.net/10138/302814
https://doi.org/10.1002/ejic.201900169

ChemPubSoc Europe

DOI: 10.1002/ejic.201900169

EurJIC European Journal of Inorganic Chemistry

Full Paper

Lewis Acids and Lewis Bases

Parallels between Metal-Ligand Cooperativity and Frustrated Lewis Pairs

Evi R. M. Habraken,[a] Andrew R. Jupp,[a] Maria B. Brands,[a] Martin Nieger,[b] Andreas W. Ehlers,[a,c] and J. Chris Slootweg*[a]

Abstract: Metal ligand cooperativity (MLC) and frustrated Lewis pair (FLP) chemistry both feature the cooperative action of a Lewis acidic and a Lewis basic site on a substrate. A lot of work has been carried out in the field of FLPs to prevent Lewis adduct formation, which often reduces the FLP reactivity. Parallels are drawn between the two systems by looking at their reactivity with CO_2, and we explore the role of steric bulk in preventing dimer formation in MLC systems.

Introduction

Over the past decades catalysis has been dominated by transition metal complexes. The partially filled d-orbitals grant the metal centre both donor and acceptor orbitals on a single atom and allow prototypical transition metal reactivity such as oxidative addition of dihydrogen, shown in Scheme 1.i, which involves an increase on the formal oxidation state of the metal by +2. In these cases, the surrounding ligands are crucial for tuning the electronic and steric properties of the metal centre, but they are not directly involved in the reactions. Separating the donor and acceptor site has led to new reaction pathways for catalysis. This reactivity occurs when the ligand actively participates in substrate activation together with the metal centre, and has been termed bifunctionality or metal-ligand cooperativity (MLC), shown in Scheme 1.ii. Noyori first demonstrated this concept with a ruthenium-phosphine complex bearing an ethylenediamine ligand, where the amine functionality cooperates with the metal.[1] In these reactions the formal oxidation state of the metal is unchanged on activation of the substrate. This topic has grown rapidly and been reviewed on many occasions,[2] and has important ramifications for catalyst design.

Another form of cooperation can be found in transition metal-free frustrated Lewis pairs (FLPs), where the acceptor and donor site are also on separate sites.[3] Lewis acids and bases typically form Lewis adducts, however incorporation of bulky groups on the donor and/or acceptor sites can induce frustration and prevent adduct formation. The unquenched reactivity of the Lewis acid and base has been exploited for the activation of small molecules, such as H_2 and CO_2, and for the subsequent catalytic hydrogenation of unsaturated substrates.[4] The Lewis acid and base can be tethered to afford an intramolecular FLP (Scheme 1.iii), which allows for preorganization of the reactive site and can reduce the (entropic) energy barrier for such activation reactions.[5,6] The interplay between the electronic and steric properties of the Lewis acids and bases is of paramount importance in determining the activity of the FLP system.

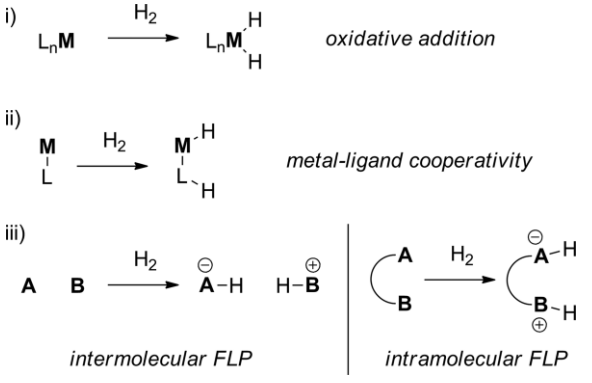

Scheme 1. Differing modes of dihydrogen activation by transition metal complexes and frustrated Lewis pairs (**M** = transition metal, **A** = Lewis acidic site, **B** = Lewis basic site, L = ligand).

The fields of FLP and MLC chemistry have both grown rapidly and, in general, separately. However, it is clear that the underlying cooperativity for the activation of substrates is similar in both cases. The distinction was further blurred by the advent of transition metal-based FLPs, where a transition metal centre is used as one of the Lewis acidic or basic sites in an FLP.[7] Wass and co-workers introduced a cationic zirconocene-phosphinoaryloxide complex, with the zirconium centre acting as a Lewis acid and a pendant phosphine acting as a Lewis base for the activation of dihydrogen (Scheme 2.i).[8] Just as with

[a] *Van 't Hoff Institute for Molecular Sciences, University of Amsterdam, Science Park 904, 1090 GD Amsterdam, The Netherlands*
E-mail: j.c.slootweg@uva.nl
[b] *Department of Chemistry, University of Helsinki, A. I. Virtasen aukio 1, PO Box 55, Helsinki, Finland*
[c] *Department of Chemistry, Science Faculty, University of Johannesburg, PO Box 254, Auckland Park, Johannesburg, South Africa*
Supporting information and ORCID(s) from the author(s) for this article are available on the WWW under https://doi.org/10.1002/ejic.201900169.

traditional main-group FLPs, the balance of sterics and electronics is important, as simply switching the $[C_5Me_5]^-$ (Cp*) ligands for $[C_5H_5]^-$ (Cp) resulted in a strong Zr–P interaction, and shut down the FLP reactivity. This reactivity could be equally well described as FLP or MLC chemistry, and Wass noted this insight in subsequent articles.[9a,9b] The analogy has also been noted elsewhere, especially with the transition metal-based FLPs,[9,10] and recently Bullock and co-workers cited guiding principles from main-group and transition metal-based FLPs in the design of bifunctional Mo complexes for the controlled heterolytic cleavage of dihydrogen (Scheme 2.ii).[11] Herein we further explore the relationships between archetypal MLC and FLP systems, and in particular investigate the dimerization of the active MLC-monomer by Lewis adduct formation, and to consolidate the knowledge garnered from the two topics.

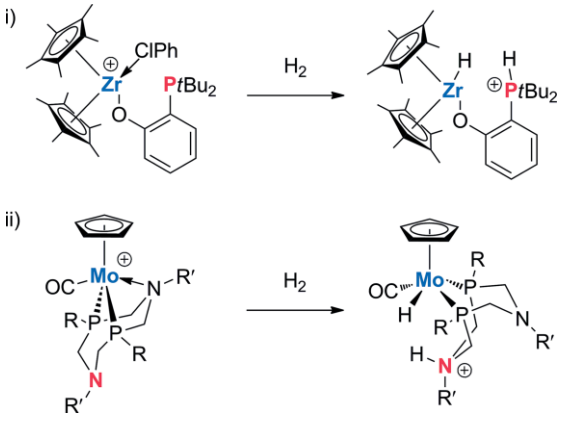

Scheme 2. Transition metal-based FLP reactivity, and/or MLC reactivity: activation of dihydrogen by i) Wass's Zr complex[8] and ii) Bullock's Mo complex.[11] Blue: Lewis acid; red: Lewis base.

Results and Discussion

We chose to investigate the quintessential Ru-based PNP pincer systems developed by Milstein, as it is well established that these species can undergo an MLC pathway via dearomatization/rearomatization of the pyridine ring.[2a] Treatment of the precursors **1** and **2**, which differ by the R group on the phosphine, with base leads to deprotonation of one of the methylene arms and loss of chloride to afford **3** and **4**, respectively (Figure 1).[12,13] These compounds feature a Lewis basic site on the carbon and a Lewis acidic site on the Ru centre. This notion was confirmed by our DFT calculations of the frontier molecular orbitals of **3** at the ωB97X-D/6-311G(d,p) level of theory, which showed that the highest occupied molecular orbital (HOMO) is principally located on the deprotonated carbon, and the lowest unoccupied molecular orbital (LUMO) is centred on the ruthenium. In this case the "frustration" of the Lewis acidic and basic sites is enforced by the rigid ligand framework. Otten and co-workers have previously demonstrated the FLP-like reactivity of a related Ru-based PNN system with nitriles,[14] in which the Ru/C combination added in a cooperative fashion across the CN triple bond. Milstein has also noted that the cooperative addition of CO_2 across these pincer systems bears a resemblance to FLPs.[10,15]

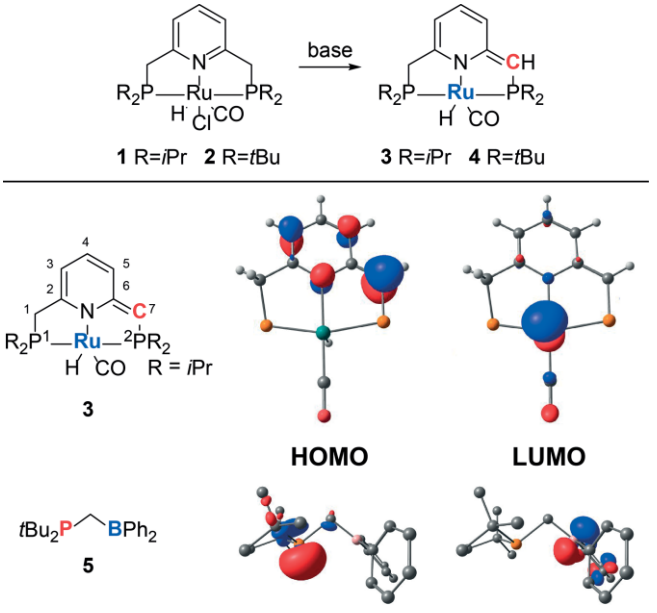

Figure 1. Top: Milstein system, activation of precursor by deprotonation with a base resulting in the dearomatized species. Bottom: molecular orbital diagram of MLC **3** (isopropyl groups omitted for clarity) and FLP **5** (left: HOMO, right: LUMO) calculated at the ωB97X-D/6-311G(d,p) level of theory. Blue: Lewis acid; red: Lewis base.

To compare this traditional MLC system with a main-group FLP, we opted to study the intramolecular FLP, **5** (Figure 1). The acidic and basic components are preorganised by the methylene bridge in the ideal orientation to activate a range of small molecule substrates, including dihydrogen, carbon dioxide and isocyanates, despite the lack of strong electron-withdrawing groups on the boron centre.[6] The HOMO is the lone pair on phosphorus, and the LUMO is predominantly the formally vacant p orbital on boron. The parallels between the orbitals of **3** and **5** should bear out in their reactivity, so we resorted to DFT calculations to provide detailed mechanistic insight into the mode of activation of carbon dioxide of the two systems.

Milstein and co-workers already partially elaborated on the activation of CO_2 for **4**,[16] which we extended to **3** to investigate the influence of the steric bulk, and this was compared to the geminal FLP system **5** (Figure 2). The latter was also investigated in the original publication, but at a different level of theory, so all calculations herein were carried out using ωB97X-D/6-311G(d,p) for ease and relevance of comparison. Pertinent bond metric data are included in Table 1, including the bond lengths between the CO_2 and the Lewis acidic and basic sites, as well as the bond lengths and angle within the CO_2 moiety. For both MLC systems, first a van der Waals complex is formed with long distances between the MLC and CO_2, and the CO_2 moiety has barely deviated from linearity. The complex is energetically favourable, but the ΔG values are slightly uphill due to a decrease in entropy. This initial complexation is followed by a nucleophilic attack by the ligand-based carbon to the carbon of CO_2 in an asynchronous concerted transition state (**3** $\Delta G^{\ddagger}$ = 3.3; **4** $\Delta G^{\ddagger}$ = 3.8 kcal mol^{-1}). In both cases the Ru–O and C–C bonds are still relatively long, indicating an early transition state. Ring closure affords the product with an overall energy

difference of ΔG = 12.1 and 10.4 kcal mol^{-1} for **3** and **4**, respectively. There is little energetic difference between the isopropyl or *tert*-butyl groups during the reaction profile, and the bond lengths (largest difference 0.03 Å) and angles (largest difference 0.6°) are similar in all cases.

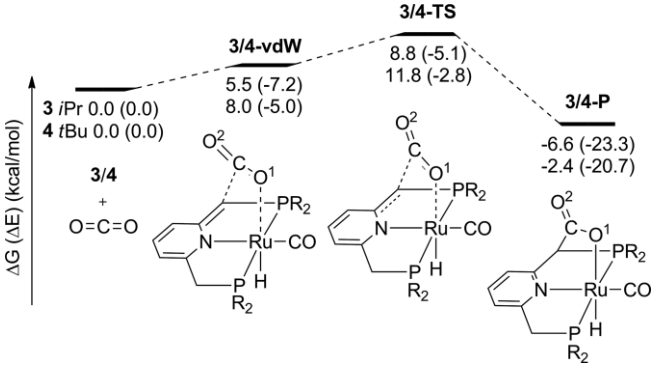

Figure 2. Relative ωB97X-D/6-311G(d,p) Gibbs free energies (energy in brackets) in kcal mol^{-1} for the reaction of CO_2 and **3**/**4**.

Table 1. Computed bond metric data for the van der Waals complexes (vdW), transition states (TS) and products (P) during the reactions of CO_2 with **3**, **4** and **5**.[a]

		LA–O^1 [Å]	LB–C^{CO2} [Å]	C–O^1 [Å]	C–O^2 [Å]	O–C–O [°]
vdW	**3**	2.55	3.14	1.16	1.15	175.9
	4	2.56	3.16	1.16	1.15	176.0
	5	3.63	3.46	1.16	1.16	177.6
TS	**3**	2.43	2.43	1.18	1.16	158.9
	4	2.45	2.42	1.18	1.16	158.3
	5	3.00	2.26	1.20	1.19	147.8
P	**3**	2.26	1.59	1.27	1.22	129.3
	4	2.29	1.59	1.27	1.22	129.1
	5	1.57	1.88	1.28	1.21	128.8

[a] LA = Lewis acid (Ru in **3**, **4**; B in **5**); LB = Lewis base (C in **3**, **4**; P in **5**).

The reaction profile for **5** is similar (Figure 3). First a van der Waals complex is formed with long distances between the FLP and CO_2 with an almost linear CO_2. The reaction proceeds via an asynchronous concerted transition state ($\Delta G^{\ddagger}$ = 12.5 kcal mol^{-1}), where the Lewis basic phosphorus centre attacks the electrophilic carbon of CO_2, and the O^1 is stabilised by interaction with the boron centre. This is evidenced by the slightly longer C–O^1 and C–O^2 bond lengths and the smaller bond O–C–O bond angle in **TS-5** than the analogous metrics in **TS-3** and **TS-4**, and is in good agreement with the previously reported bond order data for **TS-5**.[6] The final product is formed by ring closure, which is exergonic by 5.4 kcal mol^{-1}. In both the MLC and FLP systems the mechanism is the same, and differences in energies and bond metrics are readily explained by the varying electronic nature of the Lewis acidic and basic sites in the molecules.

Intramolecular FLPs can quench either via an intramolecular interaction or dimerization, although "quench" in this case is perhaps a misnomer, as it is now well established that complete frustration is not necessary for typical FLP reactivity to occur. Stephan and co-workers recently showed that even the classical adduct of $B(C_6F_5)_3$ and the strongly basic proazaphosphatrane

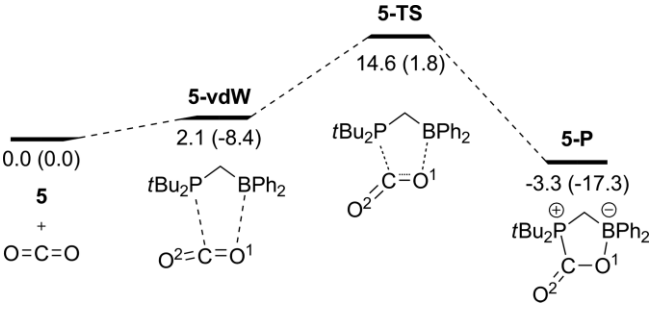

Figure 3. Relative ωB97X-D/6-311G(d,p) Gibbs free energies (energy in brackets) in kcal mol^{-1} for the reaction of CO_2 and **5**.

P[N(Me)CH_2CH_2]$_3$N is capable of addition to a range of heteroallenes.[17] In any case, the Lewis adduct is a resting state; dissociation into the corresponding Lewis acid/base components with the accompanying energy penalty is required to induce FLP reactivity. Therefore, the control of reactivity via fine-tuning of the steric environment is still a widely employed strategy in FLP chemistry. In a similar manner, MLC systems are able to dimerize via an intermolecular interaction of the Lewis acidic and Lewis basic sites in the complex. For example, the dearomatized Ru-PNS system dimerizes as shown in Figure 4, and subsequently undergoes a decomposition pathway involving C-S cleavage and loss of isobutene.[18]

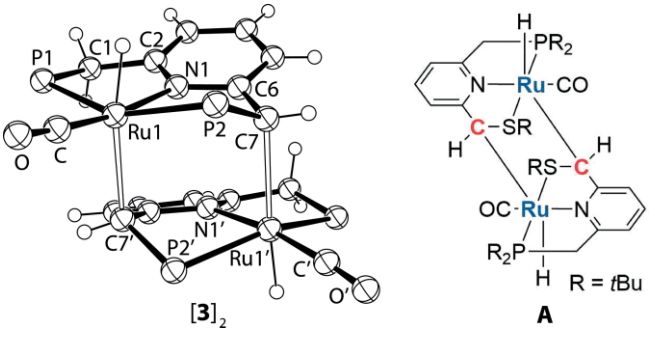

Figure 4. Two examples of dimeric MLC complexes. Left: molecular X-ray structure of [**3**]$_2$ (displacement ellipsoids are set at 50 % probability, isopropyl groups on the phosphorus are omitted for clarity).[12] Selected bond lengths [Å]: Ru1–C7′ 2.409(7), Ru1′–C7 2.403(7), P2–C7 1.797(6), C6–C7 1.456(8), C1–C2 1.489(9), C1–P1 1.842(6), P2′–C7′ 1.803(6), C6′–C7′ 1.449(8), C1′–C2′ 1.55(1), C1′–P1′ 1.843(6). Right: Milstein's Ru(PNS) dimer **A**.[18] Blue: Lewis acid; red: Lewis base.

On examination of the crystal structure of **3**, as reported in Milstein's original publication,[12] we noted that this species is also a dimer in the solid state. The ruthenium–carbon interatomic distance between the two monomers in the X-ray structure [Ru1–C7′ 2.409(7) and Ru1′–C7 2.403(7) Å] lies within the sum of the van der Waals radii (3.75 Å)[19] suggesting a bonding interaction. The C6–C7 bond lengths (according to the atom labelling in Figure 1) in [**3**]$_2$ are 1.456(8) and 1.449(8) Å. These bond lengths are much longer than that found in the gas-phase DFT optimized monomer **3** (1.379 Å), but shorter than that found in the X-ray structure of unactivated complex **1** [1.501(2) Å], which suggests that the deprotonated arm features a C–C bond with partial double bond character. In fact, the C6–C7 bond length is similar to that found in **A** [1.458(4) Å; Figure 4].[18]

To probe the structural changes that occur during dimerization, we examined the aromaticity of the pyridine ring of the compounds using NICS(0) calculations.[20,21] As expected, the unactivated precursors feature an aromatic ring (**1**: –6.4 ppm, **2**: –6.5 ppm), whereas in the activated species dearomatization has occurred (**3**: 2.0 ppm, **4**: 1.3 ppm). These values are consistent with previous studies by Gonçalves and Huang on similar organometallic pincer complexes.[22,23] Interestingly, the dimer $[\mathbf{3}]_2$ has a value (–4.7 ppm) between that of **1** and **3**, indicating partial rearomatization of the pyridine ring and a contributing factor to the stability of the dimer.

The bonding situation in $[\mathbf{3}]_2$ was further analysed using AIM analyses,[24,25] which revealed a bond critical point (BCP) between the Lewis acidic Ru site of one monomer and the Lewis basic C7 site of the other monomer [Figure 5, ρ = 0.047 a.u. (ξ = 0.21), Ru–C7 2.499 Å], indicative of a weak interaction. Furthermore, a ring critical point (RCP) is found in the dimer between the two monomers. The examination of the Laplacian of the electron densities ($\nabla^2\rho$) in the C6–C7 bond reveals a weaker interaction for the dimer than the monomer, yet still stronger than for **1** ($[\mathbf{3}]_2$: –0.66 a.u., **3**: –0.83 a.u., **1**: –0.58 a.u.). ETS-NOCV[26] analyses of the dimer, which we have used to assess donor–acceptor interactions, concur with these observations and revealed an interaction between ruthenium and the carbon in the backbone of both monomers, showing orbital interactions and specifically σ donations of 24.4 and 20.7 kcal mol^{-1} from C7 to Ru.

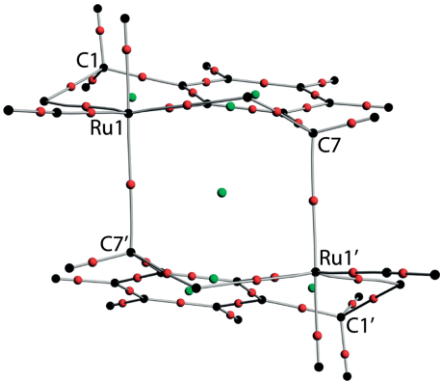

Figure 5. Computed AIM bond paths of $[\mathbf{3}]_2$, a simplified framework is depicted (isopropyl groups on P and all H atoms omitted for clarity); bond critical points (BCP) in red, ring critical points (RCP) in green.

The monomeric pincer complexes are the active species in catalysis, therefore the dimer must first be broken before it can react (Figure 6). DFT calculations at the ωB97X-D/6-311G(d,p) level of theory reveal it costs ΔG = 15.4 kcal mol^{-1} (ΔE = 29.7 kcal mol^{-1}) to break up dimer $[\mathbf{3}]_2$ (Table 2; all values given per monomer). To give a better reflection of the thermodynamics of this equilibrium in solution, we augmented our computational method by including implicit solvation effects (benzene and THF). As expected, this lowers the amount of energy required to break the dimer, the more polar solvent THF does this to a greater extent (benzene: ΔG = 13.6 kcal mol^{-1}, THF: ΔG = 12.4 kcal mol^{-1}). Explicit solvent interactions are also important, especially for monomeric species such as **3** where the Ru centre has a vacant coordination site that can be stabilised by solvent. Including one benzene molecule per monomer in the calculations lowered the energy required very slightly (ΔG = 12.8 kcal mol^{-1}), as benzene only weakly coordinates to the Ru centre in an η^2 fashion. Once again, the more coordinating THF stabilises the monomer to a greater extent, making it easier to cleave the dimer (ΔG = 5.5 kcal mol^{-1}); we anticipate that coordinating substrates will have a similar effect.

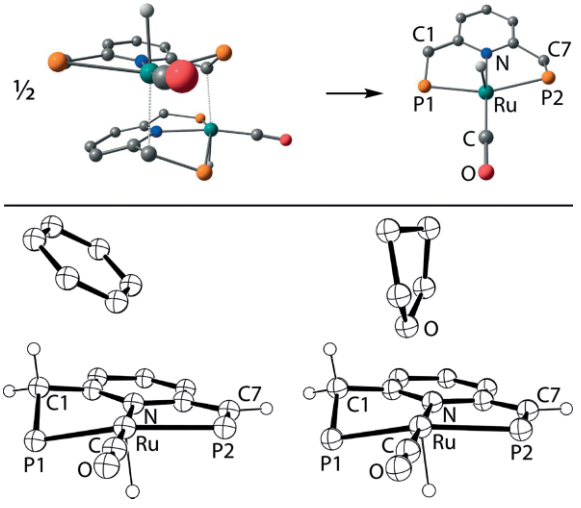

Figure 6. Top: cleavage of dimer $[\mathbf{3}]_2$ into monomer **3**. Bottom: optimized structures of **3**·THF (left, oxygen coordinates to ruthenium) and **3**·C_6H_6 (right, coordination in an η^2 fashion to ruthenium).

Table 2. Energy (ΔE) and Gibbs free energy (ΔG) required to break dimer $[\mathbf{3}]_2$ in kcal mol^{-1} (all values given per monomer).

	ΔG [kcal mol^{-1}]	ΔE [kcal mol^{-1}]
No solvent added	15.4	29.7
Implicit THF	12.4	26.4
Implicit benzene	13.6	28.1
Explicit THF added, implicit THF	5.5	14.1
Explicit benzene added, implicit Benzene	12.8	22.6

Interestingly, and reminiscent of the tenets of FLP chemistry, increasing the steric bulk of the alkyl substituents on phosphorus from isopropyl to *tert*-butyl (i.e. going from **3** to **4**) destabilises these Lewis acid/Lewis base interactions and precludes dimer formation. It was not possible to locate a minimum on the potential energy surface corresponding to the structure of $[\mathbf{4}]_2$, and all attempts led to regeneration of the two monomers during the optimization process.

To corroborate these insights on the dimerization of **3** and **4** in different solvents, we analysed the diagnostic ^{1}H NMR chemical shift of the Ru-bound hydride, both computationally and experimentally (Table 3). The computed shift for monomer **3** is approximately –20 ppm, while the corresponding shift for $[\mathbf{3}]_2$ is relatively deshielded and is computed to be approximately –10 ppm, with little dependence on the identity of the solvent. Experimentally, the hydride in benzene solutions of **3** was found to resonate at δ –13.04 ppm,[12] while in THF it is at δ –20.05 ppm. The latter is a very good match with the predicted monomeric structure, while the former is closer to the dimeric species, and suggests the existence of a monomer/dimer equilibrium. These data follow the trends predicted by the computa-

tions above, in that the quenching of the MLC is more likely to occur in less coordinating solvents such as benzene. These data are further supported by the fact that the analogous hydride in **A** (Figure 4), which is known to rapidly dimerise, resonates relatively downfield at δ –11.83 ppm in the non-coordinating solvent CD_2Cl_2.[18]

Table 3. Experimental and computational data of the hydride shift of various compounds.

Compound	Experimental data [ppm]	Computational data [ppm][a] THF[b]	Benzene[b]
3		–20.23	–19.90
3 in $[D_8]$THF	–20.05		
3 in C_6D_6	–13.04		
$[\mathbf{3}]_2$[c]		–10.16	–10.19
4		–18.58	–18.36
4 in $[D_8]$THF	–26.17		
4 in C_6D_6	–25.78		
$[\mathbf{4}]_2$		n.a.	n.a.
A in CD_2Cl_2[a]	–11.83		

[a] Calculations were performed using ωB97X-D/6-311G(d,p), Ru Def2TZVP level of theory. [b] Calculated using implicit solvent interactions; n.a. = not applicable, as the dimeric structure could not be obtained computationally. [c] Both hydrides have the same shift (–10.16 or –10.19).

The notion that the difference in the experimental chemical shift of the hydride of **3** in THF and benzene is related to dimerization is reinforced by the fact that the analogous experimental values for **4**, a system where dimerization is not possible, are very similar in the two solvents (benzene: δ –25.78 ppm; THF: δ –26.17 ppm, implicit solvent added). It should be noted that the computed values in this case are not very accurate, as they predict the resonance at approximately –18.5 ppm, depending on the solvent, and thus caution is advised in analysing the close correlation between the computed and observed values for **3** in THF above. However, the fact that the experimental values of **3** are significantly different in the two solvents, while the corresponding values for **4** are almost identical, is evidence for the presence of monomer/dimer equilibrium effects.

Finally, we wanted to show that consideration of steric bulk is important for regulating the quenching of the Lewis acid/Lewis base components in other organometallic pincer systems. Kirchner[27] and Huang[28] have replaced the methylene bridges in Milstein's PNP pincer system with the more acidic NH moiety (Figure 7).[29] Calculations at the ωB97X-D/6-311G(d,p) level of theory (with no solvent modelled) reveal a dimer is feasible for [(*i*PrP^{N}N^{N}P)RuH(CO)], and it costs ΔG = 11.3 kcal mol^{-1} to break up the dimer (per monomer), which is slightly lower than for the Milstein system. Once again, for the *tert*-butyl complex [(*t*BuP^{N}N^{N}P)RuH(CO)], the added steric protection around the acidic and basic sites prevents dimerization. However, the altered electronics of the Lewis basic site in these complexes compared to **3** and **4** have drastic consequences, as the activation of CO_2 is no longer feasible {ΔG = 15.3 and ΔG = 23.7 kcal mol^{-1} for [(*i*PrP^{N}N^{N}P)RuH(CO)] and [(*t*BuP^{N}N^{N}P)RuH(CO)], respectively}.

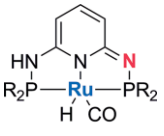

R = *i*Pr, *t*Bu

Figure 7. Representation of the activated [(R-P^{N}N^{N}P)RuH(CO)] complex, R = *i*Pr or *t*Bu. Blue: Lewis acid; red: Lewis base.

Conclusions

We have shown that FLP and MLC chemistry both involve the cooperative action of a Lewis acid and a Lewis base, and that steric control to prevent quenching of the reactive sites is just as important in both paradigms. There are many reactions in the literature that have been given one label or the other on a fairly arbitrary basis, and we believe both schools of thought should be united so that lessons from one field can be used to benefit the other – whether that is using principles and reactions from main-group FLPs to broaden the scope of MLC reactivity, or using the wealth of knowledge on ligand design and properties to rationally construct new backbones for preorganised intramolecular main-group FLPs.

Experimental Section

All manipulations regarding the preparation of air-sensitive compounds were carried out under an atmosphere of dry nitrogen using standard Schlenk and drybox techniques. Solvents were purified, dried and degassed according to standard procedures. ^{1}H NMR spectra were recorded on a Bruker AV 400 or on a Bruker AV300-II and internally referenced to the residual solvent resonances ($[D_8]$THF: ^{1}H δ 3.58, 1.72 ppm; C_6D_6: ^{1}H δ 7.16 ppm; $[D_8]$Tol: ^{1}H δ 2.08, 6.97, 7.01, 7.09 ppm). ^{31}P{^{1}H} NMR spectra were recorded on a Bruker AV 400 or on a Bruker AV300-II and externally referenced (85 % H_3PO_4). Chemical shifts are reported in ppm. High resolution mass spectra were recorded on a Bruker MicroTOF with ESI nebulizer (ESI) at –45 °C.

Synthesis of Diisopropylphosphine: Diisopropylphosphine was prepared according to a modified literature procedure of A. S. Glodman et al.[30] A solution of ClP*i*Pr$_2$ (4.92 g, 0.032 mol, 1.0 equiv.) diethyl ether (55 mL) was added dropwise to a slurry of $LiAlH_4$ (0.37 g, 0.01 mol, 0.3 equiv.) in diethyl ether (30 mL) in an ice/water bath. The mixture was stirred overnight and conversion was checked by ^{31}P{^{1}H} NMR. Degassed H_2O (20 mL) was added slowly and the organic layer was dried with $MgSO_4$. The water layer was extracted with diethyl ether (3 × 15 mL) and dried with the same $MgSO_4$. The $MgSO_4$ was filtered off (with a cannula filter) and rinsed with diethyl ether (3 × 15 mL). All volatiles were removed in vacuo while the Schlenk vessel was cooled in an ice/water bath to afford diisopropylphosphine as a colourless clear liquid in 81 % (3.08 g, 0.026 mol). If some phosphine was oxidized a Schlenk to Schlenk distillation was performed. Note, the presence of some diethyl ether does not influence the next step. ^{1}H NMR (400.1 MHz, C_6D_6, 291 K): δ = 2.93 (dt, $^1J_{H,P}$ = 192.3 Hz, $^3J_{H,H}$ = 5.9 Hz, 1H; P*H*), 1.77 (m, 2H; *CH*(CH$_3$)), 1.01 (m, 12H; CH(*CH*$_3$)). ^{31}P{^{1}H} NMR (162.0 MHz, C_6D_6, 295 K): δ = –16.5 (s).

Lithiation of Diisopropylphosphine: Lithium diisopropylphosphide was prepared according to a modified literature procedure of A. Jansen and S. Pitter.[31] *n*-Butyllithium (1.6 M in hexanes, 5.2 mL, 8.347 mmol, 1.4 equiv.) was added dropwise to a solution of diisopropylphosphine (7.045 mg, 5.962 mmol, 1.0 equiv.) in *n*-pentane

(15 mL) at 0 °C with a glass stirring bean and stirred for an additional 30 min, after which the solution was warmed to room temperature. The resulting colourless/pale yellow solution was stirred for 16 hours during which an off-white solid precipitated. The solids were collected by filtration, subsequently washed with *n*-pentane (2 × 15 mL) and the solvents evaporated to dryness to give lithium diisopropylphosphide as an off-white solid in 76 % (562.7 mg, 4.535 mmol). ^{1}H NMR (400.1 MHz, [D$_8$]THF, 297 K): δ = 2.25 (dsept, $^{2}J_{H,P}$ = 6.8 Hz, $^{3}J_{H,H}$ = 4.7 Hz, 2H; C*H*(CH$_3$)$_2$), 1.07 (dd, $^{2}J_{H,P}$ = 11.3 Hz, $^{3}J_{H,H}$ = 6.8 Hz, 12H; CH(C*H*$_3$)$_2$). ^{7}Li NMR (155.5 MHz, [D$_8$]THF, 297 K): 1.3 (s). ^{13}C NMR (100.6 MHz, [D$_8$]THF, 297 K): δ = 26.93 (d, $^{3}J_{C,P}$ = 14.2 Hz; CH(*C*H$_3$)$_2$), 23.4 (d, $^{2}J_{C,P}$ = 25.3 Hz; *C*H(CH$_3$)$_2$). ^{31}P{^{1}H} NMR (162.0 MHz, [D$_8$]THF, 297 K): δ = 1.5 (s).

Preparation of 2,6-Bis(diisopropylphosphino-methyl)-pyridine: 2,6-Bis(diisopropylphosphino-methyl)-pyridine was prepared according to a modified literature procedure of A. Jansen and S. Pitter.[31] A solution of 2,6-bis(chloromethyl)pyridine (0.26 g, 1.477 mmol, 1.0 equiv.) in THF (2.0 mL) as added slowly to a solution of the lithiated phosphine (0.40 g, 3.223 mmol, 2.2 equiv.), using a glass stirring bean, in THF (4.0 mL) at –78 °C and was stirred for an additional 15 min at the same temperature. During the addition, the solution changed colour from yellow to orange, and subsequently was warmed to room temperature in 16 h. Addition of degassed water (0.2 mL) resulted in a colour change to yellow and the mixture was dried with Na_2SO_4. The solution was filtered and the Na_2SO_4 was washed with THF (3 × 4 mL). The combined solution was dried in vacuo, extracted with pentane (3 × 5 mL) and the solvents evaporated to dryness to give ***i*PrPNP** as a yellow oil in 88 % (0.44 mg, 1.296 mmol, 95 % pure). Note, some remaining diisopropylphosphine can be observed. ^{1}H NMR (400.1 MHz, C$_6$D$_6$, 298 K): δ = 7.13–7.04 (m, 1H; *p*-Py*H*), 7.02–6.95 (m, 2H; *m*-Py*H*), 2.97 (d, $^{2}J_{H,P}$ = 1.5 Hz, 4H; C*H*$_2$), 1.71 (dsept, $^{2}J_{H,P}$ = 7.1, 1.7 Hz, 4H; C*H*(CH$_3$)$_2$), 1.05 (m, 24H; CH(C*H*$_3$)$_2$). ^{31}P{^{1}H} NMR (162.0 MHz, C$_6$D$_6$, 297 K): δ = 11.4 (s; product, 95 %), –12.1 (s; impurity, presumably *i*Pr$_2$PH, 5 %).

Synthesis of 1. [(*i*PrPNP)RuHCl(CO)] was prepared according to a literature procedure.[32] X-ray quality crystals were grown at –20 °C from a saturated solution of **[(*i*PrPNP)RuHCl(CO)]** in THF layered with *n*-pentane.

Synthesis of 2. [(*t*BuPNP)RuHCl(CO)] was prepared according to a literature procedure.[13]

Synthesis of 3. [(*i*PrPNP)RuH(CO)] was prepared according to a slightly modified literature procedure.[12] To a solution of complex [(*i*PrPNP)RuHCl(CO)] **1** (50 mg, 0.099 mmol) in THF (5 mL) was added KO*t*Bu (11.1 mg, 0.099 mmol) at –30 to –35 °C. Subsequently, the mixture was stirred at room temperature for 4 h, then filtered. The orange filtrate was dried under vacuum and washed with *n*-pentane (3 × 3 mL) and dried under vacuum to afford a yellowish powder in 56 % yield (26 mg, 0.055 mmol).

Synthesis of 4. [(*t*BuPNP)RuH(CO)] was prepared according to a literature procedure.[13]

X-ray Crystal Structure Determination: The single-crystal X-ray diffraction study (see Figure 8) was carried out on a Bruker D8 Venture diffractometer with Photon100 detector at 123(2) K using Mo-K_α radiation (l = 0.71073 Å). Dual space (intrinsic) methods (SHELXT)[33] were used for structure solution and refinement was carried out using SHELXL-2014 (full-matrix least-squares on F^2).[34] Hydrogen atoms were localized by difference electron density determination and refined using a riding model [H(Ru) free]. A semi-empirical absorption correction and an extinction correction were applied.

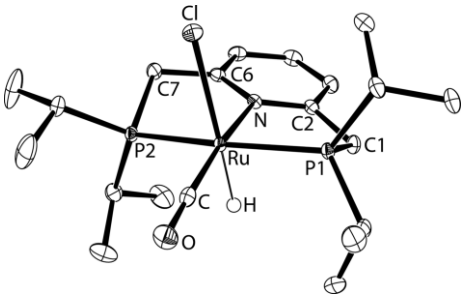

Figure 8. Molecular structure of **1** [(*i*PrPNP)RuHCl(CO)] (displacement ellipsoids are set at 50 % probability, hydrogen atoms omitted for clarity). Selected bond lengths [Å]: Ru–P1 2.3221(4), Ru–P2 2.3061(4), P1–C1 1.8415(14), P2–C7 1.8435(15), C1–C2 1.5051(19), C6–C7 1.501(2).

1: Colourless blocks, $C_{20}H_{36}ClNOP_2Ru$, M_r = 504.96, crystal size 0.24 × 0.18 × 0.10 mm, monoclinic, space group $P2_1/c$ (No. 14), a = 13.7461(6) Å, b = 11.7625(5) Å, c = 14.4290(7) Å, β = 95.022(2)°, V = 2324.05(18) Å^3, Z = 4, ρ = 1.443 Mg/m^{-3}, μ(Mo-K_α) = 0.94 mm^{-1}, F(000) = 1048, $2\theta_{max}$ = 55.2°, 50402 reflections, of which 5365 were independent (R_{int} = 0.034), 239 parameters, R_1 = 0.019 [for 4830 $I > 2\sigma(I)$], wR_2 = 0.044 (all data), S = 1.06, largest diff. peak/hole = 0.35/–0.49 e Å^{-3}.

CCDC 1884053 (for **1**) contains the supplementary crystallographic data for this paper. These data can be obtained free of charge from The Cambridge Crystallographic Data Centre.

Computational Details: Density functional calculations were performed at the ωB97X-D[35] level of theory using Gaussian09, revision D.01.[36] Geometry optimizations were performed using the 6-311G(d,p)[37] basis set for atoms C, H, N, O, P, Cl, in combination with the Def2TZVP[38] basis set for Ru. ZPE and Gibbs free energies (G°) were obtained from frequency analyses performed at the same level of theory. Calculations of large dimer systems with solvation (SCRF, THF or benzene) were obtained from frequency analyses after optimization without solvation. The NICS[39] analyses was performed at the ωB97X-D/6-311G(d,p), Ru Def2TZVP//B3LYP[40]/6-311G(d,p), Ru Def2TZVP level of theory. The AIM[41] and ETS-NOCV[42] analyses were performed at the ZORA-BP86/TZ2P[42] level of theory using ADF2016.102.[42] Structures were optimized using the same functional and basis set prior to the analysis using ZORA-BP86/TZ2P. NMR calculations were performed at ωB97X-D/6-311G(d,p), Ru Def2TZVP level of theory, using solvation (THF or benzene) and are corrected for the TMS value[39,43] and obtained with the Gauge-Independent Atomic Orbital (GIAO).[44]

Acknowledgments

This work was supported by the Council for Chemical Sciences of The Netherlands Organization for Scientific Research (NWO/CW) by a VIDI grant (J. C. S.) and a VENI grant (A. R. J.). We gratefully acknowledge Ed Zuidinga for mass spectrometric analyses.

Keywords: Lewis acids · Lewis bases · Frustrated Lewis pairs · Metal ligand cooperativity · Density functional calculations

[1] T. Ohkuma, H. Ooka, S. Hashiguchi, T. Ikariya, R. Noyori, *J. Am. Chem. Soc.* **1995**, *117*, 2675–2676.
[2] a) J. R. Khusnutdinova, D. Milstein, *Angew. Chem. Int. Ed.* **2015**, *54*, 12236–12273; *Angew. Chem.* **2015**, *127*, 12406; b) M. Trincado, H. Grützmacher

in *Cooperative Catalysis: Designing Efficient Catalysts for Synthesis* (Ed.: R. Peters), Wiley-VCH, Weinheim, **2015**, p. 67–110; c) H. Valdés, M. A. García-Eleno, D. Canseco-Gonzalez, D. Morales-Morales, *ChemCatChem* **2018**, *10*, 3136-3172; d) C. Gunanathan, D. Milstein, *Acc. Chem. Res.* **2011**, *44*, 588–602; e) H. Grützmacher, *Angew. Chem. Int. Ed.* **2008**, *47*, 1814–1818; *Angew. Chem.* **2008**, *120*, 1838; f) C. Gunanathan, D. Milstein, *Chem. Rev.* **2014**, *114*, 12024–12087.

[3] G. C. Welch, R. R. San Juan, J. D. Masuda, D. W. Stephan, *Science* **2006**, *314*, 1124–1126.

[4] a) F.-G. Fontaine, D. W. Stephan, *Phil. Trans. R. Soc. A* **2017**, *375*, 20170004; b) G. Kehr, S. Schwendemann, G. Erker, *Top. Curr. Chem.* **2012**, *332*, 45–84; c) D. J. Scott, M. J. Fuchter, A. E. Ashley, *Chem. Soc. Rev.* **2017**, *46*, 5689–5700; d) D. W. Stephan, *J. Am. Chem. Soc.* **2015**, *137*, 10018–10032.

[5] a) P. Spies, G. Erker, G. Kehr, K. Bergander, R. Fröhlich, S. Grimme, D. W. Stephan, *Chem. Commun.* **2007**, 5072–5074; b) C. M. Mömming, E. Otten, G. Kehr, R. Fröhlich, S. Grimme, D. W. Stephan, G. Erker, *Angew. Chem. Int. Ed.* **2009**, *48*, 6643–6646; *Angew. Chem.* **2009**, *121*, 6770.

[6] F. Bertini, V. Lyaskovskyy, B. J. J. Timmer, F. J. J. de Kanter, M. Lutz, A. W. Ehlers, J. C. Slootweg, K. Lammertsma, *J. Am. Chem. Soc.* **2012**, *134*, 201–204.

[7] Examples of complexes where the metal is the Lewis base: a) J. Campos, *J. Am. Chem. Soc.* **2017**, *139*, 2944–2947; b) W. H. Harman, J. C. Peters, *J. Am. Chem. Soc.* **2012**, *134*, 5080–582; c) S. J. K. Forrest, J. Clifton, N. Fey, P. G. Pringle, H. A. Sparkes, D. F. Wass, *Angew. Chem. Int. Ed.* **2015**, *54*, 2223–2227; *Angew. Chem.* **2015**, *127*, 2251.

[8] a) A. M. Chapman, M. F. Haddow, D. F. Wass, *J. Am. Chem. Soc.* **2011**, *133*, 8826–8829; b) A. M. Chapman, M. F. Haddow, D. F. Wass, *J. Am. Chem. Soc.* **2011**, *133*, 18463–18478.

[9] a) S. R. Flynn, D. F. Wass, *ACS Catal.* **2013**, *3*, 2574–2581; b) D. F. Wass, A. M. Chapman, *Top. Curr. Chem.* **2013**, *334*, 261–280; c) D. W. Stephan, G. Erker, *Angew. Chem. Int. Ed.* **2015**, *54*, 6400–6441; *Angew. Chem.* **2015**, *127*, 6498; d) D. W. Stephan, *Science* **2016**, *354*, aaf7229; e) M. T. Whited, *Beilstein J. Org. Chem.* **2012**, *8*, 1554–1563; f) R. M. Bullock, G. M. Chambers, *Phil. Trans. R. Soc. A* **2017**, *375*, 20170002.

[10] For more papers drawing an analogy between MLCs and TM-FLPs, see: a) A. T. Normand, C. G. Daniliuc, B. Wibbeling, G. Kehr, P. L. Gendre, G. Erker, *J. Am. Chem. Soc.* **2015**, *137*, 10796–10808; b) A. N. Marziale, A. Friedrich, I. Klopsch, M. Drees, V. R. Celinski, J. S. auf der Günne, S. Schneider, *J. Am. Chem. Soc.* **2013**, *135*, 13342–13355; c) B. Askevold, H. W. Roesky, S. Schneider, *ChemCatChem* **2012**, *4*, 307–320; d) M. J. Sgro, D. W. Stephan, *Chem. Commun.* **2013**, *49*, 2610–2612; e) A. Pal, K. Vanka, *Dalton Trans.* **2013**, *42*, 13866–13873; f) S. Arndt, M. Rudolph, A. S. K. Hashmi, *Gold Bull.* **2017**, *50*, 267–282; g) N. P. Mankad, *Chem. Commun.* **2018**, *54*, 1291–1302.

[11] S. Zhang, A. M. Appel, R. M. Bullock, *J. Am. Chem. Soc.* **2017**, *139*, 7376–7387.

[12] J. Zhang, G. Leitus, Y. Ben-David, D. Milstein, *Angew. Chem. Int. Ed.* **2006**, *45*, 1113–1115; *Angew. Chem.* **2006**, *118*, 1131.

[13] B. Gnanaprakasam, J. Zhang, D. Milstein, *Angew. Chem. Int. Ed.* **2010**, *49*, 1468–1471; *Angew. Chem.* **2010**, *122*, 1510.

[14] L. E. Eijsink, S. C. P. Perdriau, J. G. de Vries, E. Otten, *Dalton Trans.* **2016**, *45*, 16033–16039.

[15] M. Feller, U. Gellrich, A. Anaby, Y. Diskin-Posner, D. Milstein, *J. Am. Chem. Soc.* **2016**, *138*, 6445–6454.

[16] M. Vogt, M. Gargir, M. A. Iron, Y. Diskin-Posner, Y. Ben-David, D. Milstein, *Chem. Eur. J.* **2012**, *18*, 9194–9197.

[17] T. C. Johnstone, G. N. J. H. Wee, D. Stephan, *Angew. Chem. Int. Ed.* **2018**, *57*, 5881–5884; *Angew. Chem.* **2018**, *130*, 5983.

[18] M. Gargir, Y. Ben-David, G. Leitus, Y. Diskin-Posner, L. J. W. Shimon, D. Milstein, *Organometallics* **2012**, *31*, 6207–6214.

[19] a) S. S. Batsanov, *Inorg. Mater.* **2001**, *37*, 871–885; b) S. S. Batsanov, *Inorg. Mater.* **2001**, *37*, 1031–1046.

[20] Z. Chen, C. S. Wannere, C. Corminboeuf, R. Puchta, P. von Ragué Schleyer, *Chem. Rev.* **2005**, *105*, 3842–3888.

[21] NICS calculations were performed using ωB97X-D/6-311G(d,p), Ru Def2TZVP//B3LYP/6-311G(d,p), Ru Def2TZVP level of theory where NICS(0) is calculated in the ring centre. Negative values of NICS(0) correspond to aromaticity, positive values to antiaromaticity and small negative or positive values to non-aromaticity.

[22] T. Gonçalves, K.-W. Huang, *J. Am. Chem. Soc.* **2017**, *139*, 13442–13449.

[23] For more aromatization/dearomatization of PNP pincer ligands, see: a) T. Simler, G. Frison, P. Braunstein, A. A. Danopoulos, *Dalton Trans.* **2016**, *45*, 2800–2804; b) M. Feller, E. Ben-Ari, M. A. Iron, Y. Diskin-Posner, G. Leitus, L. J. W. Shimon, L. Konstantinovski, D. Milstein, *Inorg. Chem.* **2010**, *49*, 1615–1625.

[24] R. F. W. Bader, *Atoms in Molecules*, Claredon Press, Oxford, **1994**.

[25] The AIM analysis was performed at BP86/TZ2P, Ru ZORA using ADF2016.102; see ESI for details.

[26] M. P. Mitoraj, A. Michalak, T. Ziegler, *J. Chem. Theory Comput.* **2009**, *5*, 962–975.

[27] D. Benito-Garagorri, E. Becker, J. Wiedermann, W. Lackner, M. Pollak, K. Mereiter, J. Kisala, K. Kirchner, *Organometallics* **2006**, *25*, 1900–1913.

[28] L.-P. He, T. Chen, D.-X. Xue, M. Eddaoudi, K.-W. Huang, *J. Organomet. Chem.* **2012**, *700*, 202–206.

[29] H. Li, B. Zheng, K.-W. Huang, *Coord. Chem. Rev.* **2015**, *293–294*, 116–138.

[30] K. Zhu, P. D. Achord, X. Zhang, K. Krogh-Jespersen, A. S. Goldman, *J. Am. Chem. Soc.* **2004**, *126*, 13044–13053.

[31] A. Jansen, S. Pitter, *Monatsh. Chem.* **1999**, *130*, 783–794.

[32] J. Zhang, G. Leitus, Y. Ben-David, D. Milstein, *J. Am. Chem. Soc.* **2005**, *127*, 10840–10841.

[33] G. M. Sheldrick, *Acta Crystallogr., Sect. A* **2015**, *71*, 3–8.

[34] G. M. Sheldrick, *Acta Crystallogr., Sect. C* **2015**, *71*, 3–8.

[35] J.-Da. Chai, M. Head-Gordon, *Phys. Chem. Chem. Phys.* **2008**, *10*, 6615–6620.

[36] M. J. Frisch, G. W. Trucks, H. B. Schlegel, G. E. Scuseria, M. A. Robb, J. R. Cheeseman, G. Scalmani, V. Barone, B. Mennucci, G. A. Petersson, H. Nakatsuji, M. Caricato, X. Li, H. P. Hratchian, A. F. Izmaylov, J. Bloino, G. Zheng, J. L. Sonnenberg, M. Hada, M. Ehara, K. Toyota, R. Fukuda, J. Hasegawa, M. Ishida, T. Nakajima, Y. Honda, O. Kitao, H. Nakai, T. Vreven, J. A. Montgomery Jr., J. E. Peralta, F. Ogliaro, M. Bearpark, J. J. Heyd, E. Brothers, K. N. Kudin, V. N. Staroverov, R. Kobayashi, J. Normand, K. Raghavachari, A. Rendell, J. C. Burant, S. S. Iyengar, J. Tomasi, M. Cossi, N. Rega, J. M. Millam, M. Klene, J. E. Knox, J. B. Cross, V. Bakken, C. Adamo, J. Jaramillo, R. Gomperts, R. E. Stratmann, O. Yazyev, A. J. Austin, R. Cammi, C. Pomelli, J. W. Ochterski, R. L. Martin, K. Morokuma, V. G. Zakrzewski, G. A. Voth, P. Salvador, J. J. Dannenberg, S. Dapprich, A. D. Daniels, Ö. Farkas, J. B. Foresman, J. V. Ortiz, J. Cioslowski, D. J. Fox, *Gaussian 09, Revision D.01*, Gaussian, Inc., Wallingford CT, **2013**.

[37] a) A. D. McLean, G. S. Chandler, *J. Chem. Phys.* **1980**, *72*, 5639–5648; b) K. Raghavachari, J. S. Binkley, R. Seeger, J. A. Pople, *J. Chem. Phys.* **1980**, *72*, 650–654; c) J.-P. Blaudeau, M. P. McGrath, L. A. Curtiss, L. Radom, *J. Chem. Phys.* **1997**, *107*, 5016–5021; d) A. J. H. Wachters, *J. Chem. Phys.* **1970**, *52*, 1033–1036; e) P. J. Hay, *J. Chem. Phys.* **1977**, *66*, 4377–4384; f) K. Raghavachari, G. W. Trucks, *J. Chem. Phys.* **1989**, *91*, 1062–1065; g) R. C. Binning Jr., L. A. Curtiss, *J. Comput. Chem.* **1990**, *11*, 1206–1216; h) M. P. McGrath, L. Radom, *J. Chem. Phys.* **1991**, *94*, 511–516; i) L. A. Curtiss, M. P. McGrath, J.-P. Blaudeau, N. E. Davis, R. C. Binning Jr., L. Radom, *J. Chem. Phys.* **1995**, *103*, 6104–6113.

[38] a) F. Weigend, R. Ahlrichs, *Phys. Chem. Chem. Phys.* **2005**, *7*, 3297–3305; b) F. Weigend, *Phys. Chem. Chem. Phys.* **2006**, *8*, 1057–1065.

[39] J. Gauss, *Chem. Phys. Lett.* **1992**, *191*, 614–620.

[40] A. D. Becke, *J. Chem. Phys.* **1993**, *98*, 5648–5652.

[41] a) J. I. Rodríguez, R. F. W. Bader, P. W. Ayers, C. Michel, A. W. Götz, C. Bo, *Chem. Phys. Lett.* **2009**, *472*, 149–152; b) J. I. Rodríguez, *J. Comput. Chem.* **2013**, *34*, 681–686.

[42] a) G. te Velde, F. M. Bickelhaupt, S. J. A. van Gisbergen, C. Fonseca Guerra, E. J. Baerends, J. G. Snijders, T. Ziegler, *J. Comput. Chem.* **2001**, *22*, 931–967; b) C. Fonseca Guerra, J. G. Snijders, G. te Velde, E. J. Baerends, *Theor. Chem. Acc.* **1998**, *99*, 391–403; c) ADF2016, SCM, Theoretical Chemistry, Vrije Universiteit, Amsterdam, The Netherlands, http://www.scm.com.

[43] J. R. Cheeseman, G. W. Trucks, T. A. Keith, M. J. Frisch, *J. Chem. Phys.* **1996**, *104*, 5497–5509.

[44] a) F. London, *J. Phys. Radium* **1937**, *8*, 397–409; b) R. McWeeny, *Phys. Rev.* **1962**, *126*, 1028–1034; c) R. Ditchfield, *Mol. Phys.* **1974**, *27*, 789–807; d) K. Wolinski, J. F. Hilton, P. Pulay, *J. Am. Chem. Soc.* **1990**, *112*, 8251–8260; e) Ref. [43].

Received: February 13, 2019